Fabrication of Large–Area Polymeric Membranes with Micro and Nano Aperatures

K. Li[1], J.A. Hernández-Castro[1,2] and T. Veres[1,2]

[1]National Research Council of Canada, 75, de Montagne, Boucherville (Québec), J4B 6Y4, Canada
Kebin.li@nrc.gc.ca
[2]Biomedical Engineering Department, McGill University, 3775 University Street, Montréal, Québec, H3A 2B4, Canada

ABSTRACT

A group of membranes of different materials, including radical and cationic UV lacquer, PFPE urethane methacrylate UV resin (MD700), optical adhesive UV resin with high refractive index (NOA84), as well as thermally curable polydimethylsiloxane (PDMS) have been successfully fabricated by using a simple, yet robust method. The membranes are replicated from an intermediate template with micro- or nano-pillars by using the spontaneous capillary flow (SCF) method. The polymerization is done either by UV or thermal curing. The size of the pores in the membrane ranges from 100 µm down to 200 nm. The thickness of the membranes varies from 10 µm up to 100 µm. As high as 16 of aspect ratio (the thickness of the membrane to the diameter of the pore) has been achieved in membranes with thickness of 100 µm and 6 µm pore diameter. Uniform open-through hole membranes with pore size of 15 µm and thickness of 30 µm over an area of 44×44 mm^2 have also been achieved.

Keywords: Nanoimprinting, UV polymerization, Micro /nano fabrication, Micromolding, Spontaneous Capillary flow

1 INTRODUCTION

Micro- and nano-porous membranes have a wide range of applications, including plasmonics, data storage, and energy devices, as well as biomedical devices. Most of them use silicon, silicon nitride, or highly periodic anodic alumina membranes[1-5]. These membranes are mechanically stable and offer the advantage of maintaining the membrane's shape against external forces that arise during the handling process, but they are fragile and brittle.

Alternatively, flexible polymeric membranes are relatively less expensive to fabricate and offer several advantages, such as conformal wetting and easy peel-off without significant damage and distortion. They are getting more and more attractive for biological applications[6-8]. However it is non-trivial to make polymeric membranes with regular, straight, open-through pores because it is quite challenging to obtain 'freestanding' and 'residual-layer-free' structures in the fabrication of polymeric membranes, especially as pore sizes get smaller[9]. Here, we present a simple yet robust method for polymer membrane fabrication, which could be scaled up eventually.

2 EXPERIMENT

2.1 Process of Polymeric Membranes Fabrication

Figure 1 shows the general process flow chart for the fabrication of polymeric membranes by using an intermediate template. The cavities of the template with multiscale micro/nano pillars are filled by polymeric resin via spontaneous capillary flow (SCF). The polymerization is done by UV or thermal curing. Separation of the cured membrane from the template is performed under solvent. For most cases presented here, the template is made of polyvinyl alcohol (PVA) and therefore it is eventually dissolved into deionized (DI) water to release the polymeric membrane from the template. Alternatively, the separation of polymeric membranes from the template could be done under a polar solvent like methanol for a certain group of polymers, this will be discussed in detail later on. The PDMS mold is replicated from a Si master (with Si posts) fabricated by using a deep reactive ion etching (DRIE) method based on standard photolithography processes. The surface of the PDMS mold was coated with a monolayer of trichlorol(1H, 1H, 2H, 2H)-perfluorooctyl-silane (97%) (Sigma-Aldrich, Oakville, ON) by placing it under vacuum in a desiccator for two hours. The template scaffold was replicated in PVA (Sigma-Aldrich) from the PDMS mold. The PVA solution was made by dissolving 20 wt. % of PVA, which has a hydrolysis degree of 89% and a molecular weight of about 100000g mol^{-1}, in water. The PVA solution was then poured over the PDMS mold and vacuum was then applied for an hour to remove air bubbles, followed by slow drying in an oven at 50^{o} C. For easy handling, the thickness of the PVA template is preferred to be more than 300 µm. The replicated PVA template was then detached from the PDMS mold without any sticking issues.

2.2 Polymer Resin Filling by Capillary Force

In order to fill the PVA scaffold with polymer, two strategies could be applied. For example, one can use the vacuum assisted micro-molding method presented in

MicroTas 2016[10]. Alternatively, one can also fill the PVA scaffold by capillary force. It can simplify the fabrication process and can be potentially scaled up in a mass production fashion.

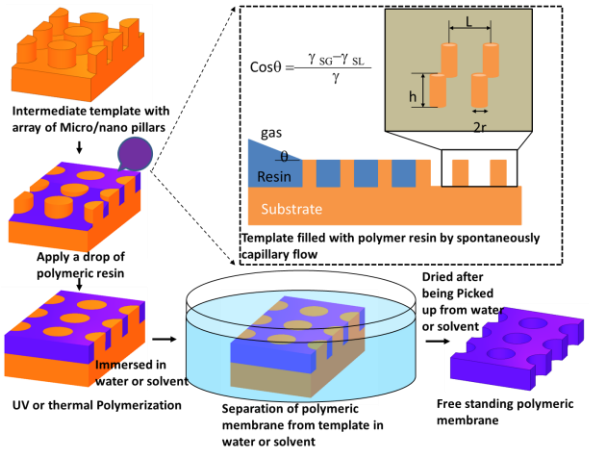

Figure 1: Process flow chart for making polymeric membranes via an intermediate template by SCF filling method. Insert depicts the flow of polymer on a micro structured PVA surface with an array of micro pillars with height of *h*, radius of *r*, and period of *L*.

Casavant et al.[11] reported that liquid can propagate spontaneously along a micro channel, even without floor and ceiling (suspended flow), by capillary force if the internal pressure P, which is the variation of free energy per unit volume dE/dV, at the liquid front is negative.

$$P = \frac{dE}{dV} = \gamma_{LG}\left(\frac{dA_{LG}}{dV} - \cos\theta \frac{dA_{SL}}{dV}\right)$$

Where dA is the variation in areas, with the indices *L*, *S*, and *G* representing liquid, solid, and gas phases, respectively. θ is the contact angle of the fluid on the solid surface, γ_{LG} is the surface energy of the fluid between liquid and gas with the reservoir pressure being zero. For an open system with an array of posts (diameter of 2*r* and height of *h*) with period of *L* arranged in a square pattern, given that the condition for flow is $P < 0$, the condition for SCF can be written as:

$$\frac{L^2-\pi r^2}{L^2-\pi r^2+2\pi rh} < \cos\theta \qquad \text{Eq.(1)}$$

Since the left side of Eq.(1) is always smaller than 1, the above equation holds true as long as the contact angle is small enough. It's well known that the hydrophilicity of the resin filling is enhanced by the micro-structure, namely, it requires the value of the left side of Eq.(1), determined by the geometry of the micro-structured template, to be as small as possible. For example, if the item $2\pi rh$ is comparable to L^2-πr^2, that means it requires certain density of pillars on the one hand and the height of the pillar should be comparable to or larger than the diameter of the pillars (with aspect ratio (height/diameter) larger than 1) on the other hand. As long as these basic requirements are met, the cavity of a PVA scaffold could be simply and automatically filled with polymeric resin by SCF.

2.3 Fabrication of Polymeric Membrane in Various Materials

Once a PVA scaffold with an array of pillars is ready, a drop of UV resin is put into a groove surrounding the structured PVA pillars, the cavities of the PVA scaffold will be automatically filled with the polymeric resin. After all the cavities of the PVA scaffold have been filled with polymeric resin, it is cured by UV exposure at room temperature for one minute with a flood lamp UV-curing system (Dymax ECE 2000UV, Torrington, USA). The PVA template is then dissolved in water, assisted with ultrasonic agitation, for about 5 minutes, and the separated membrane is finally picked up from the water and placed on a glass slide for characterization later on.

Fig. 2(B) shows the SEM image of the bottom side of a fabricated membrane which replicated the surface of the PVA scaffold at the bottom of the pillars, whose SEM image is shown in Fig. 2(A). The membrane is made of CUVR1534 resin, which is a mixture of UVACURE 1500 (from Allnex Canada Inc., Ontario, Canada) and CAPA™ 3035 (from Perstrop Sweden), in a ratio of 50:50 by weight. It also shows the cross section of the membrane, this clearly demonstrates that the holes are straight and open-through, the diameter of the pores is approximately 16 µm. The top side surface of the membrane is shown in Fig. 2(C).

A goup of polymer membranes have been successfully fabricated with different materials, such as the free radical UV resin EBECRY 3708 (50% in TPGDA by weight) from Cytec (Allnex Canada Inc., Ontario, Canada), MD700 (Solvay Solexis MD700 (PFPE urethane methacrylate) added with 1% Darcure1173 photo-initiator), optical adhesive UV resins with high refractive index, *e.g.* NOA84 (Norland Products Inc., NJ), and medical adhesive UV resins, *e.g.* 1161-M (Dymax Co.) whose SEM image is shown in Fig.2(E). It is also found that PDMS can spontaneously fill the PVA cavities, although the filling speed is not as fast as for the UV resins. A PDMS membrane with hole size of 5 µm in diamter, shown in Fig.2(D), was also fabricated.

Fig.2(F) shows a photo of one piece of CUVR1534 membrane with thickness of 30 µm and pore size of 15 µm, over area of 44×44 mm^2, the pores are arranged in square configuration with a pitch size of 30 µm. We have also successfully fabricated a membrane with 15 µm holes arranged in a honeycomb configuration, the distance between two adjacent pores is fixed at 22 µm, which gives us a 42% porosity in this specific membrane design. The aspect ratio (AR) of the membrane's thickness over pore diamter is eventually limited by the AR of the PVA microposts used in the process, which in turn is determined by the Si master mold and the mold replication process. Fig. 2(G) and (H) are the SEM images of the bottom side and top side of a NOA84 membranes replicatedd from the PVA

pillars. The surface topology of the membranes around the holes on the bottom side has a micro concave shape, which is formed on the Si master during the DRIE process. The cross section view of the images shows that the diameter of the holes on top of the membrane is slightly smaller than at the bottom, this is especially obvious when the size of the structures is getting smaller, and it's caused by over etching of the top of the pillars during the DRIE process as well. The diamter of the holes is approximately 6 µm and the thickness of the membrane is 100 µm, which results in an AR of 16.

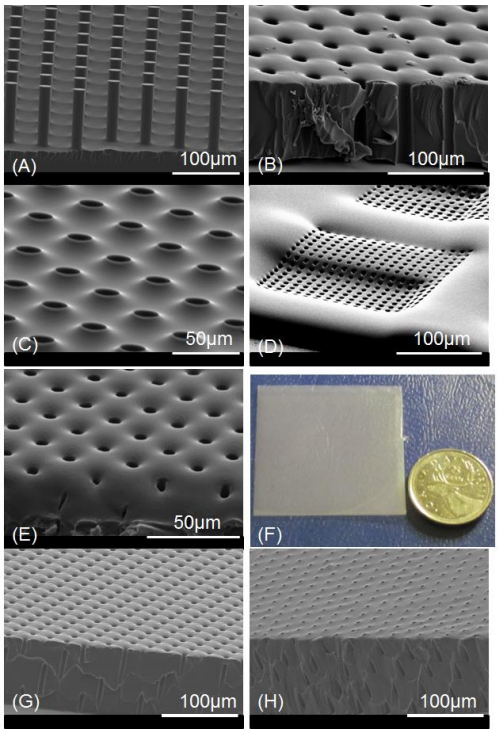

Figure 2: SEM images of a PVA mold (A) and a fabricated CUVR1534 membrane with thickness of 80 µm and over an area of 16×33 mm^2 (B and C). (D) SEM image of the top side of a PDMS membrane. (E) SEM image of the top side of a 1161-M membrane. (F) Photo of a CUVR1534 membrane with thickness of 30 µm and over a 44×44 mm^2 area. (G, H) SEM images of the bottom and top side of a NOA84 membrane with AR of 16.

2.4 Fabrication of Polymeric Membranes with Nano Apertures

In order to make polymer membranes with nano apertures, it is very useful to apply the strategy of geometric reinforcement via multiple scales and multilevel architectures in the process. We designed a master mold with combination of nano- and microstructures. The Si master mold was fabricated by both e-beam lithography and photolithography processes. An array of square Si nanopillars (10×10 mm^2 patterned area) with 300 nm by side and 600 nm in height, arranged in a honeycomb configuration (the distance of a pillar to the nearest six surrounding pillars is fixed at 600 nm) was fabricated by e-beam lithography. It was then integrated with an array of micropillars (44×44 mm^2 patterned area). The micropillars, with diameter of 15 µm and pitch size of 30 µm, were arranged in a square configuration and fabricated by photolithography. The height of the micropillars was 30 µm and constructed by DRIE. After the process, it forms a Si master mold with micropillars in an area of 44×44 mm^2, where it includes a 10×10 mm^2 area array of complex pillars (nanopillars on top of a micropillar).

The nanostructures on the Si master mold could be well-replicated on a Zeonor substrate via hot-embossing, with an intermediate working stamp (WS) replication step (MD700 UV cured polymer). Fig. 3(A, B) show SEM images of the hot-embossed Zeonor 1060R substrate, showing that the complex pillars are well-replicated from the fabricated Si master mold. An array of square nanopillars, with dimensions from 220 to 240 nm by side (they're smaller than the designed value 300 nm because the metal mask was over etched during the fabrication process, the square shape is also slightly rounded after the processing) and 600 nm high, sitting on top of a micropillar whose diameter and height are 15 µm, and 30 µm, respectively. But there are some defective nanopillars (smaller, shorter, sometimes broken or tilted), especially close to the edge of the micropillars, these defects are probably due to damage caused during mold transfer steps (from Si master to WS stamp mold), or during the demolding process after hot-embossing. The sub-microstructures that appear around the 15 µm pillars as well as on the floor among the pillars are attributed to the effects of the DRIE process.

Zeonor 1060R is a type of cyclic olefin copolymer (COC) which has good resistance to most chemicals, like acids, bases, and polar solvents, but poor against nonpolar solvents, like hexane, toluene, and oils. It is hard to use Zeonor 1060R as a sacrificial substrate to make polymer membranes by the method described above because it is hard to find a chemical which can partially or totally dissolve this COC without or with limited attack to the polymer used for the membrane fabrication. However, some polar solvents can cause swelling, but without permanent damage to the polymer. In this case, instead of dissolving the sacrificial substrate in solvent, the swelling of the polymer membrane in some specific solvent can facilitate the cured polymer to separate from the Zeonor scaffold. UV cured CUVR1534 is one of such kind of polymers, which swells when it is immersed in methanol.

Fig.3 (C) shows the surface of the bottom side of the membrane, it looks somewhat rough, or porous. This resulted from the presence of some sub-microstructuredpins on the fabricated Zeonor mold. They are not open-through because the height of those pins is less than 5 µm, as shown in Fig.3(A).

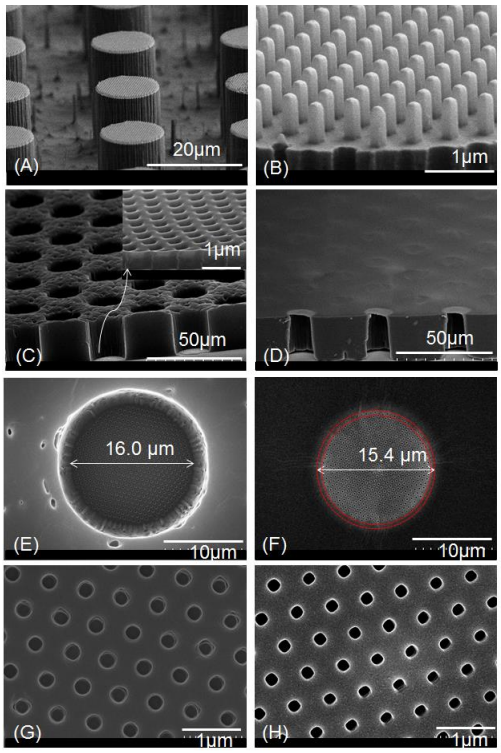

Fig.3 (A) SEM image of a hot-embossed Zeonor 1060R substrate with a combination of nanopillars on micropillars. (B) Close-up of the SEM image shown in (A). (C) and (D) SEM images (tilt at 70º) of a CUVR1534 membrane with combination of nano/micro open-through holes (shown from bottom and top sides, respectively). Insert in (C) is the cross section view of the membrane with nanoholes. (E) and (F) are elevated view SEM images of the membrane from the bottom and top side, respectively. (G) to (H) are the SEM images of (E) and (F) at higher magnifications.

From the cross section view of the microholes, it is found that the sub-micrometer features on the wall of the microholes are well-replicated from the features found on the Zeonor pillars, shown in Fig.3(A). The microhole is covered by a very thin layer on the other end, under a high magnification view, as shown in the insert of Fig. 3(C), the thickness of this thin membrane layer is found to be approximately 550 nm, which is highly consistent with the height of the nano pillars shown in Fig.3 (B), and these holes are seen to be open-through. Fig.3(D) is a SEM image of the membrane viewed at a tilt angle (70º), the top side of the membrane is facing up. From this cross section view, now the 15 μm holes are closed by a thin layer membrane on top while they are opened on the bottom side. Under high magnification, again, it is found that the sub-micrometer holes are open-through. Fig.3 (E) and (F) are elevated views SEM images of the membranes from above for the bottom and top sides, respectively. There is the impression that the diameter of the microholes at the bottom is significantly bigger than at the top. Under higher magnification, the diameter of the microhole at the top side should be "bigger" than it appears in Fig. 3(F), it includes the ring marked by dashed red lines. The contrast of this ring is darker than that of the area enclosed by the small dashed red line circle because the thinner layer in this area is not open-through, which is consistent with the SEM image of the pillars shown in Fig.3(A and B). After this correction, the diameter of the micro hole at the top side is about 15.4 μm, which is slightly smaller than that (16 μm) at the bottom side. There is also a smaller difference in the dimensions of nano holes between the bottom and top sides. The SEM images shown in Fig.3(G) and (H) indicate that the diameter of the open-through hole at the bottom side is around 250 nm (rounded square) while it is about 200 nm to 210 nm at the top. Some size variations at the top side were also observed, pores are slightly smaller around the edge than in the central region. It is probably due to the non-uniformity (variation in height, tip of a pillar getting rounded and smaller, etc.) of the nanopillars replicated from the Si master, as mentioned previously.

3 CONCLUSION

A simple yet robust method has been developed for the fabrication of freestanding polymeric membranes with micro and nanoapertures. The strategy of filling the polymer into the cavities of the template scaffold is based on the simple and powerful spontaneous capillary flow. Polymerization is done either by UV or thermal curing. Because of the advantages of the present method in many aspects of the process, transparent and flexible polymer membranes in a quite broad range of materials, with high aspect ratio (16), high porosity (42%), over large area (44×44 mm^2) have been successfully fabricated.

REFERENCES

[1] S. Aksu, AA. Yanik, R. Adato, et al., Nano. Lett, 10, 2511, 2010
[2] X. M. Yan, A. M. Contreras, M. M. Koebel, et al., Nano Lett. 5, 1129, 2005
[3] O. Vazquez et al., Nano Lett. 8, 3675, 2008
[4] W. Lee, H. Han, L. Andrity et al., Nature Nanotechnology, 30, 402, 2008.
[5] Z. Fan, H. Razavi, J. W. Do et al., Nat. Mater. 8, 648, 2009
[6] D. Huh, B. D. Matthews, A. Mammoto et al.,, Science 328, 1662, 2010
[7] K. J. Jang, K. Y. Suh, Lab Chip, 10, 36, 2010
[8]Y. Tang, J. Shi, S. Li et al., Sci. Rep. 4, 1, 2014
[9] H. Cho, J. Kim, H. Park et al., Nature Commun. 5, 3137, 2014
[10] J.A. Hernández-Castro, K. Li, A. Meunier, T. Veres, D. Juncker, MicroTAS 2016 Dublin, Ireland. Oct 9-13, 2016
[11] B. P. Casavant, E. Berthier, A. B. Theberge et al., Proc. Natl. Acad. Sci. 110, 10111, 2013.